Efficiency and Optimal Loads Analysis for Multiple-Receiver Wireless Power Transfer Systems

Minfan Fu, *Student Member, IEEE,* Tong Zhang, Chengbin Ma, *Member, IEEE,* Xinen Zhu*, *Member, IEEE*

***Abstract*—Wireless power transfer has shown revolutionary potential in challenging the conventional charging method for consumer electronic devices. Through magnetic resonance coupling, it is possible to supply power from one transmitter to multiple receivers simultaneously. In a multiple-receiver system, the overall system efficiency highly depends on the loads and receivers' positions. This paper extends the conventional circuit-model-based analysis for one-receiver system to investigate a general one-transmitter multiple-receiver system. It discusses the influence of the loads and mutual inductance on the system efficiency. The optimal loads, the input impedance and power distribution are analyzed and used to discuss the proper system design and control methods. Finally, systems with different number of receivers are designed, fabricated and measured to validate the proposed method. Under the optimal loading conditions an efficiency above 80% can be achieved for a system with three different receivers working at 13.56 MHz.**

***Index Terms*—Wireless power transfer, multiple receivers, efficiency analysis, optimal loads**

I. Introduction

WIRELESS Power Transfer (WPT) makes it possible to cut the last wire for electrical devices and provides great convenience for use. Currently, there are mainly three popular WPT technologies, including far-filed radiation [1], [2], inductive coupling [3], and magnetic resonance coupling [4], [5], with their distinguished contributions in different areas. Each technology has its own features on work frequency, power level, and transmission range [6]. Among these technologies, wireless power transfer using magnetic resonance coupling is capable to deliver power with more efficiency than far-field method, and in longer range than inductive coupling. In order to built a well-performed WPT system based on magnetic resonance coupling, many research groups have made significant contributions in different areas, such as, high efficiency dc-ac power sources [7], [8], analysis and modeling of coupling systems [9]–[14], optimum load control [15], [16], high efficiency coupling system design [17], [18], magnetic shield [19] and proper system design and control methods [20]–[25]. All these achievements can work well for a one-receiver system, however, there are still many unsolved problems to apply these techniques for a multiple-receiver system.

Supplying power for multiple loads is one of the most attractive advantages besides eliminating the last wire. A practical application scenario will be a single charging platform supplying power for various electronic devices, such as wearable devices, mobile phones, and laptops. These devices are usually different in size, power requirement, and charging condition. Thus it is a challenging task to fulfill the aforementioned situation. Over the past few years there have been several research work to address such a multiple-receiver WPT system from different perspectives. [26] used the coupled mode theory (CMT) to explore the effect of multiple devices on the overall power transfer efficiency. It showed this efficiency could be improved by adding more receivers. While other groups tend to use equivalent circuit models to analyze the same system because it is more straightforward and easily understood. In 2000, [27] used the circuit model to analyze a multiple-receiver system for high power low frequency application. They investigated the system sensitivity, the power transfer capability and controllability. However, in their model, the receiving coils are identical and have the same mutual inductances to the transmitting coil. Besides, the load variation is not considered in the system analysis. [28] provided a method to design the circuit parameters with different receivers. Also they discussed the potential to compensate the efficiency drop by resonant frequency tracking when more receivers are added. The frequency tracking can improve the overall performance. However it cannot control the power delivered to each individual receiver and its associated efficiency. [29] discussed the power distribution for a two-receiver system. But their model does not consider the effects of parasitic resistances of coils, which overestimates the system efficiency. In [30] we show the existence of optimal load conditions to achieve a maximum efficiency for a one-transmitter two-receiver WPT system. The work of this paper extends the analysis of [30] for a general one-transmitter multiple-receiver system under fixed frequency. In such a system, the receiving coils have different sizes and different mutual inductances to the transmitting coil. It carries out a general discussion about the influence of the mutual inductances instead of any specific placement for coils. The parasitic resistances are taken into consideration to accurately predict the efficiency and loading effect. The optimal loads and source for multiple receivers have been strictly proved based on the study of two-receiver systems. Moreover dynamic power distribution to each receiver can be achieved through the load control effectively. Besides, the cross coupling effects are discussed and validated in both simulation and experiment. To authors' best knowledge this is the first work to solve a practical multiple-receiver WPT system with different receiver properties.

The paper is organized in the following way. In Section II, a general system structure is given with the system efficiency definition. Then the circuit-model-based numerical analysis is carried out for one-receiver, two-receiver and finally a general

This paper is an expanded version from the IEEE MTT-S Wireless Power Transfer Conference, Jeju, Korea, May 8-9, 2014

multiple-receiver system. It gives the expression for overall system efficiency, strictly proves the existence of optimal loads, and discusses the input impedance and power distribution condition. In Section III, based on coils' parameters, a two-receiver system is used as an example to help discuss the control strategies and cross coupling effects. Then in Section IV, various experiments are designed and carried out to validate the analytical results. Finally the conclusion is drawn in Section V.

II. System Analysis

A. System Configuration

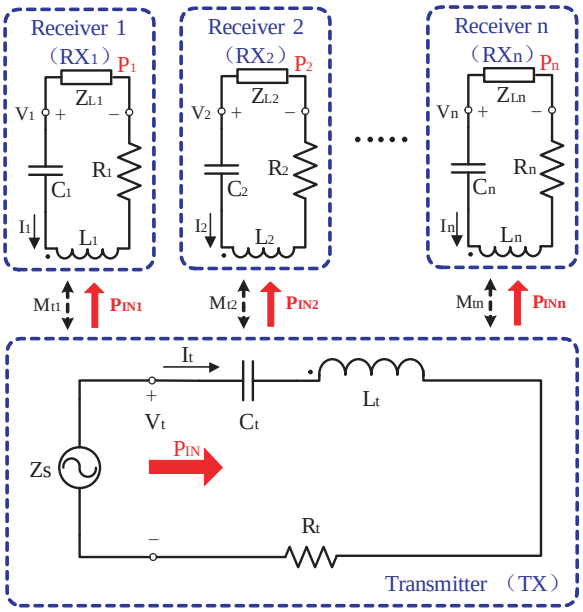

Fig. 1. Multiple-receiver WPT system configuration.

Fig. 1 shows the basic configuration for a multiple-receiver WPT system, where TX and RX are used to represent the transmitter and receiver respectively. The system consists of a TX and n RXs. At the TX side, a transmitting coil is driven by a power source with source impedance Z_s, and L_t, C_t and R_t are the inductance, capacitance and parasitic resistance of the transmitting coil. At the RX side, L_i, C_i, and R_i are the inductance, capacitance, and parasitic resistance of the ith receiving coil, and each receiving coil is followed by a resistive load Z_{Li}. M_{ti} is the mutual inductance between the transmitter and the ith receiver. The resonance is achieved by

$$j\omega L_t + \frac{1}{j\omega C_t} = 0, \tag{1}$$

$$j\omega L_i + \frac{1}{j\omega C_i} = 0, i \in [1, n]. \tag{2}$$

The efficiency for each load is

$$\eta_i = \frac{P_i}{P_{IN}}, \tag{3}$$

where P_i is the power consumed by Z_{Li} and P_{IN} is the input power to the transmitting coil. For each load, the input power is first transformed to the coupled power P_{INi} with a transmitting efficiency η_{TXi} at the TX side (some loss on R_t), and then the coupled power is further transferred to the corresponding load Z_{Li} with a receiving efficiency η_{RXi} (some loss on R_i). Therefore, the efficiency for each load can be represented as a product form,

$$\eta_i = \eta_{TXi}\eta_{RXi}, \tag{4}$$

where

$$\eta_{TXi} = \frac{P_{INi}}{P_{IN}}, \tag{5}$$

and

$$\eta_{RXi} = \frac{P_i}{P_{INi}}. \tag{6}$$

Finally, the overall system efficiency is

$$\eta = \frac{\sum_{i=1}^{n} P_i}{P_{IN}} = \sum_{i=1}^{n} \eta_i. \tag{7}$$

The following subsections first review and discuss the optimal loads for one-receiver and two-receiver system with numerical method. Then the method is extended to analyze a general multiple-receiver system.

B. One-Receiver System

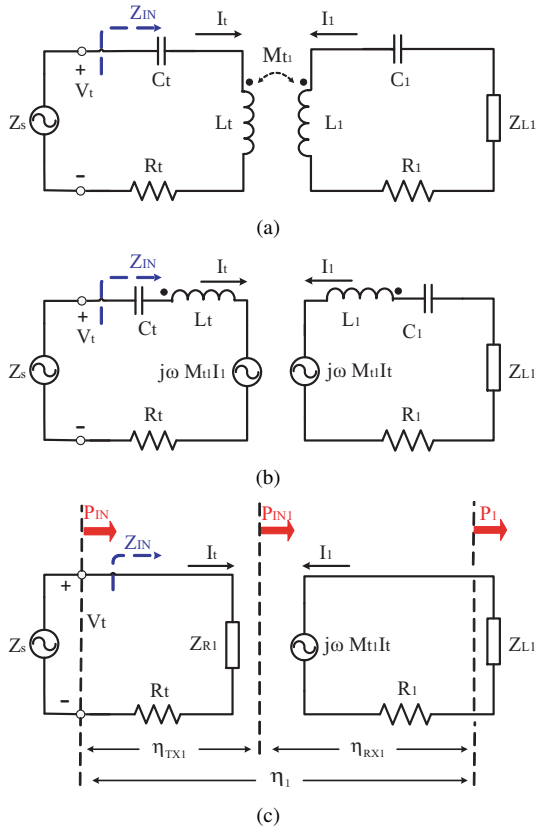

Fig. 2. One-receiver WPT system. (a) Circuit model. (b) Equivalent circuit model. (c) Circuit model under resonance.

One receiver is a fundamental structure for WPT applications. As shown in Fig. 2(a), it includes a power source, a transmitting coil, a receiving coil and a load Z_{L1}. Using

a standard mutual inductance coupling transformer model, the induced voltage in the receiver due to the transmitter current I_t is equal to $j\omega M_{t1} I_t$, while the reflected voltage in the transmitter due to the receiver current I_1 is equal to $j\omega M_{t1} I_1$. Fig. 2(b) shows this equivalent circuit model. With the Kirchhoff voltage laws (KVL), the following equations can be obtained,

$$\begin{cases} I_t(R_t + \frac{1}{j\omega C_t} + j\omega L_t) + I_1 j\omega M_{t1} - V_t = 0 \\ I_1(Z_{L1} + R_1 + \frac{1}{j\omega C_1} + j\omega L_1) + I_t j\omega M_{t1} = 0 \end{cases}. \tag{8}$$

Under resonance, I_t and I_1 can be solved as

$$\begin{cases} I_t = \frac{(Z_{L1}+R_1)V_t}{R_t(Z_{L1}+R_1)+\omega^2 M_{t1}^2} \\ I_1 = -\frac{j\omega M_{t1} V_t}{R_t(Z_{L1}+R_1)+\omega^2 M_{t1}^2} \end{cases}. \tag{9}$$

The loading effect of the receiver on the transmitter can be represented by a reflected impedance Z_{R1},

$$Z_{R1} = \frac{j\omega M_{t1} I_1}{I_t} = \frac{\omega^2 M_{t1}^2}{R_1 + Z_{L1}}. \tag{10}$$

Thus the circuit model can be simplified as shown in Fig. 2(c). The input impedance is

$$Z_{IN} = R_t + Z_{R1} = R_t + \frac{\omega^2 M_{t1}^2}{R_1 + Z_{L1}}. \tag{11}$$

The transmitting efficiency is

$$\eta_{TX1} = \frac{Z_{R1}}{R_t + Z_{R1}}. \tag{12}$$

The receiving efficiency is

$$\eta_{RX1} = \frac{Z_{L1}}{R_1 + Z_{L1}}. \tag{13}$$

Thus the system efficiency is

$$\eta = \eta_1 = \eta_{TX1}\eta_{RX1} = \frac{Z_{R1}\frac{Z_{L1}}{R_1+Z_{L1}}}{R_t + Z_{R1}}. \tag{14}$$

The optimal Z_{L1}, for a maximum η, can be calculated by taking the first-order derivative of η, and then it gives

$$Z_{L1,OPT} = R_1\sqrt{1 + \frac{\omega^2 M_{t1}^2}{R_t R_1}}. \tag{15}$$

With this optimal load, the corresponding input impedance is

$$Z_{IN,OPT} = R_t\sqrt{1 + \frac{\omega^2 M_{t1}^2}{R_t R_1}}. \tag{16}$$

Seen from the source, for no power reflection, it requires

$$Z_{S,OPT} = Z_{IN,OPT}^*. \tag{17}$$

Let

$$A_1 = \sqrt{1 + \frac{\omega^2 M_{t1}^2}{R_t R_1}}, \tag{18}$$

then $Z_{L1,OPT} = R_1 A_1$ and $Z_{S,OPT} = R_t A_1$. It can be observed that

$$Z_{S,OPT} : Z_{L1,OPT} = R_t : R_1. \tag{19}$$

Besides, under the optimal load, the maximum efficiency can be calculated and simplified as

$$\eta_{OPT} = \frac{A_1 - 1}{A_1 + 1}. \tag{20}$$

C. Two-Receiver System

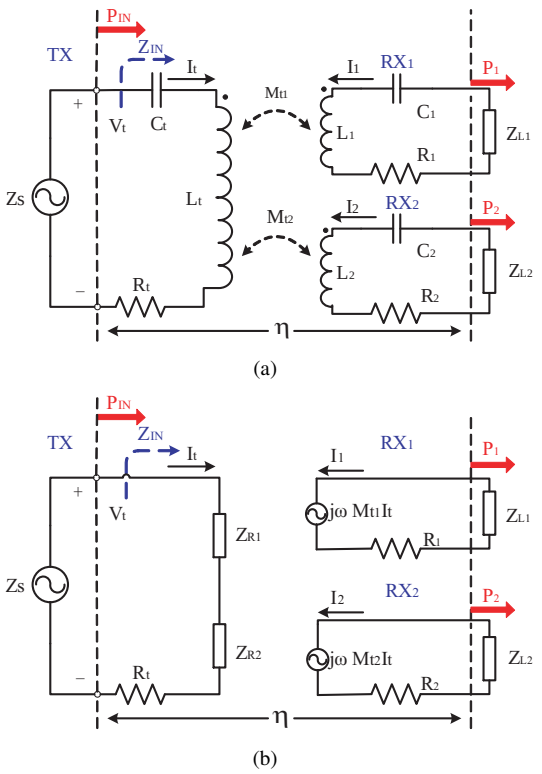

Fig. 3. Two-receiver WPT system. (a) Circuit model. (b) Circuit model under resonance.

Fig. 3(a) shows a two-receiver WPT system, which is the most fundamental multiple-receiver system. Similar to the derivation in Section II-B, three KVL functions can be applied and solved to get the relationships between I_t, I_1 and I_2. Under resonance, the circuit model can be simplified by the reflected impedances with

$$Z_{R1} = \frac{\omega^2 M_{t1}^2}{R_1 + Z_{L1}}, \tag{21}$$

and

$$Z_{R2} = \frac{\omega^2 M_{t2}^2}{R_2 + Z_{L2}}, \tag{22}$$

refer to (10). And the simplified circuit model under resonance is shown in Fig. 3(b). Based on this model, the input impedance is

$$Z_{IN} = R_t + \sum_{i=1}^{2} Z_{Ri}. \tag{23}$$

The transmitting efficiency and receiving efficiency for each load is

$$\eta_{TXi} = \frac{Z_{Ri}}{R_t + \sum_{i=1}^{2} Z_{Ri}}, \tag{24}$$

and

$$\eta_{RXi} = \frac{Z_{Li}}{R_i + Z_{Li}}, \tag{25}$$

for i=1, 2. The system efficiency is

$$\eta = \sum_{i=1}^{2} \eta_{TXi}\eta_{RXi} = \frac{\sum\limits_{i=1}^{2} Z_{Ri}\frac{Z_{Li}}{R_i+Z_{Li}}}{R_t + \sum\limits_{i=1}^{2} Z_{Ri}}. \tag{26}$$

The optimal loads for maximum η can be obtained by solving the two partial derivative equations,

$$\begin{cases} \frac{\partial \eta}{\partial Z_{L1}} = 0 \\ \frac{\partial \eta}{\partial Z_{L2}} = 0 \end{cases}. \tag{27}$$

The solution is

$$\begin{cases} Z_{L1,OPT} = R_1\sqrt{1 + \frac{\omega^2 {M_{t1}}^2}{R_t R_1} + \frac{\omega^2 {M_{t2}}^2}{R_t R_2}} \\ Z_{L2,OPT} = R_2\sqrt{1 + \frac{\omega^2 {M_{t1}}^2}{R_t R_1} + \frac{\omega^2 {M_{t2}}^2}{R_t R_2}}. \end{cases} \tag{28}$$

Similar to the one-receiver system [refer to (18)], let

$$A_2 = \sqrt{1 + \frac{\omega^2 {M_{t1}}^2}{R_t R_1} + \frac{\omega^2 {M_{t2}}^2}{R_t R_2}}, \tag{29}$$

then

$$\begin{cases} Z_{L1,OPT} = R_1 A_2 \\ Z_{L2,OPT} = R_2 A_2 \end{cases}. \tag{30}$$

Substituting these two optimal loads into (23), it has

$$Z_{S,OPT} = Z^*_{IN,OPT} = R_t A_2, \tag{31}$$

and

$$Z_{S,OPT} : Z_{L1,OPT} : Z_{L2,OPT} = R_t : R_1 : R_2. \tag{32}$$

The optimal efficiency [refer to (26)] can be calculated and simplified as

$$\eta_{OPT} = \frac{A_2 - 1}{A_2 + 1}, \tag{33}$$

which is similar to (20).

D. Multiple-Receiver System

The same numerical method can be applied for the multiple-receiver system as used in Section II-B and II-C. Assume there are n receivers, thus a (n+1) ports network can be given and described by its impedance matrix (34) [refer to Fig. 1]. Taking $Z_{Li} = -V_i/I_i$ into the first n rows of (34) can give

$$I_i = -\frac{j\omega M_{ti} I_t}{R_i + Z_{Li}}, i \in [1, n]. \tag{35}$$

Since $Z_{IN} = V_t/I_t$, taking (35) into the last row of (34) gives

$$Z_{IN} = R_t + \sum_{i=1}^{n} Z_{Ri}. \tag{36}$$

where

$$Z_{Ri} = \frac{j\omega M_{ti} I_i}{I_t} = \frac{\omega^2 {M_{ti}}^2}{R_i + Z_{Li}}. \tag{37}$$

And Z_{Ri} is the reflected impedance of RX_i on TX like Fig. 2(c) and Fig. 3(b). The transmitting and receiving efficiency for the ith load is

$$\eta_{TXi} = \frac{Z_{Ri}}{R_t + \sum\limits_{i=1}^{n} Z_{Ri}}, \tag{38}$$

and

$$\eta_{RXi} = \frac{Z_{Li}}{R_i + Z_{Li}}. \tag{39}$$

Thus the efficiency for the ith load is

$$\eta_i = \frac{Z_{Ri}\frac{Z_{Li}}{R_i+Z_{Li}}}{R_t + \sum\limits_{i=1}^{n} Z_{Ri}}. \tag{40}$$

Finally the system efficiency is

$$\eta = \frac{\sum\limits_{i=1}^{n} Z_{Ri}\frac{Z_{Li}}{R_i+Z_{Li}}}{R_t + \sum\limits_{i=1}^{n} Z_{Ri}}. \tag{41}$$

In order to derive the optimal values for n loads, a s-traightforward method is to solve n partial derivative equations simultaneously like (27). However, it is complicated to solve them directly. Instead, by observing the optimal loads for one-receiver system and two-receiver system [refer to (15) and (28)], the results are of the same form. Therefore, for a multiple-receiver system, it is reasonable to assume that the optimal load for the ith receiver is

$$Z_{Li,OPT} = R_i A_n, \tag{42}$$

where

$$A_n = \sqrt{1 + \sum_{i=1}^{n} \frac{\omega^2 {M_{ti}}^2}{R_t R_i}}, \tag{43}$$

[refer to (18) and (29)]. The sufficient conditions for the optimal loads are

$$\frac{\partial \eta}{\partial Z_{Li}} = 0, \ i \in [1, \ n]. \tag{44}$$

Applying (44) to (41), it has

$$\frac{R_i - Z_{Li}}{R_i + Z_{Li}} = \frac{-\sum\limits_{j=1}^{n} \frac{\omega^2 {M_{tj}}^2 Z_{Lj}}{(R_j+Z_{Lj})^2}}{(R_t + \sum\limits_{j=1}^{n} \frac{\omega^2 {M_{tj}}^2}{R_j+Z_{Lj}})}. \tag{45}$$

Substituting (42) into the left side of (45), (45) becomes

$$\frac{1 - A_n}{1 + A_n} = \frac{-\sum\limits_{j=1}^{n} \frac{\omega^2 {M_{tj}}^2 Z_{Lj}}{(R_j+Z_{Lj})^2}}{(R_t + \sum\limits_{j=1}^{n} \frac{\omega^2 {M_{tj}}^2}{R_j+Z_{Lj}})}. \tag{46}$$

It can be proved that (43) is the solution of (46). In sum, (42) and (43) satisfy (44), thus the assumption is true for the multiple-receiver system. With the optimal values,

$$Z_{S,OPT} = Z^*_{IN,OPT} = R_t A_n, \tag{47}$$

and

$$\eta_{OPT} = \frac{A_n - 1}{A_n + 1}. \tag{48}$$

The power flow management among different loads is another important issue in a multiple-receiver WPT system.

$$\begin{bmatrix} V_1 \\ V_2 \\ \vdots \\ V_n \\ V_t \end{bmatrix} = \begin{bmatrix} R_1 & 0 & \cdots & 0 & j\omega M_{t1} \\ 0 & R_2 & \cdots & 0 & j\omega M_{t2} \\ \vdots & \vdots & \ddots & \vdots & \vdots \\ 0 & 0 & \cdots & R_n & j\omega M_{tn} \\ j\omega M_{t1} & j\omega M_{t2} & \cdots & j\omega M_{tn} & R_t \end{bmatrix} \begin{bmatrix} I_1 \\ I_2 \\ \vdots \\ I_n \\ I_t \end{bmatrix} \tag{34}$$

With a given input power P_{IN}, power ratio between any two receiver can be represented as

$$\frac{P_i}{P_j} = \frac{\eta_i}{\eta_j} = \frac{M_{ti}^2 (R_j + Z_{Lj})^2 Z_{Li}}{M_{tj}^2 (R_i + Z_{Li})^2 Z_{Lj}},\ i, j \in [1,\ n]. \tag{49}$$

It shows that a receiver can share more power by getting closer to the transmitter or properly controlling the loads when the parasitic resistances are fixed.

In order to have more insights about the multiple-receiver WPT system, the equivalent system model will be derived. By observing (20) and (48), it finds that any multiple-receiver WPT system can be represented as an equivalent one-receiver system. Choose

$$A_{EQ} = \sqrt{1 + \frac{{M_{EQ}}^2}{R_t R_{EQ}}}, \tag{50}$$

and let $A_{EQ} = A_n$, which gives

$${M_{EQ}}^2 = \frac{\sum_{k=1}^{n} \frac{1}{R_k} {M_{tk}}^2}{\sum_{j=1}^{n} \frac{1}{R_i}}, \tag{51}$$

and

$$R_{EQ} = R_1 \parallel R_2 \cdots \parallel R_n. \tag{52}$$

A special case is that a multiple-receiver WPT system has n identical receivers with the same coupling to the transmitter, i.e., $M_{ti} = M_{SAME}$ for i $\in$ [1, n]. Then its equivalent model has $M_{EQ} = M_{SAME}$, and $R_{EQ} = R_{SAME}/n$, where R_{SAME} is the parasitic resistance of each receiving coil. It shows that if a one-receiver system is replaced by a multiple-receiver system, the system efficiency can be improved due to the reduction of equivalent parasitic resistance.

Based on above derivation, for a general multiple-receiver WPT system, following conclusions can be made:

1) The optimal loads and corresponding optimal source impedance satisfy that

$$Z_{S,OPT} : Z_{L1,OPT} : ... Z_{Ln,OPT} = R_t : R_1 : ... R_n, \tag{53}$$

which is defined as the optimal impedance ratio in this paper.

2) Under the optimal condition, all the loads share the same receiving efficiency, i.e.,

$$\eta_{RXi} = \frac{Z_{Li,OPT}}{R_i + Z_{Li,OPT}} = \frac{A_n}{A_n + 1}. \tag{54}$$

3) The overall system efficiency is proportional to A_n. So higher efficiency can be achieved by increasing the coupling between the transmitter and receivers, lowing the parasitic resistance of coils or increasing the number of receivers.
4) The power distribution among receivers can be controlled by the loads.
5) A multiple-receiver system can be represented by an equivalent one-receiver system.

III. Examples and Discussion

The numerical analysis in Section II focuses on the power transfer in the coupling system, i.e., from the transmitting coil to the receiving coils. In a complete WPT system, the transmitting coil is driven by a power source, and each receiving coil is followed by a rectifier. A dc-dc converter following the rectifier can be used to achieve load control [16]. Sometimes, an impedance matching network is required after the power source to reduce power reflection [31]. Therefore, when discussing the transfer characteristics of the coupling system, it is indispensable to evaluate the interactive relationships between the coupling system and other subsystems. The influence of the coupling system can be analyzed by its input impedance (seen by the power source) and the loads (seeing into the rectifier). Finally, a whole system design optimization can be conducted instead of subsystem improvements.

Here, a two-receiver coupling system is used as an example in circuit-model-based simulation to illustrate more details. Fig. 4(a) shows the system structure, i.e., one transmitter (TX) in the middle with two different sizes receivers (RX_1 and RX_2) at either side. The coils' sizes are given in Fig. 4(b), which is fabricated and used in the final experiment. The distance between the transmitter and each receiver is d. Meanwhile, all the coils are tuned to resonate at 13.56 MHz with external series capacitors. Using a vector network analyzer (VNA), the coils' parameters and the mutual inductances between coils are measured and summarised in Table I and II. It shows the mutual inductance between the receivers (M_{12}) is much smaller than M_{t1} and M_{t2}. Therefore, it is reasonable to ignore the influence of M_{12}. Based on the parameters and the numerical analysis in Section II, the optimal loads and the input impedance will be illustrated and discussed in the following parts.

TABLE I
Coils' parameters

	Large coil	Small coil
Parasitic resistance (Ω)	2.05	1.04
Inductance (μH)	3.93	2.01
Capacitance (pF)	37.2	72.5

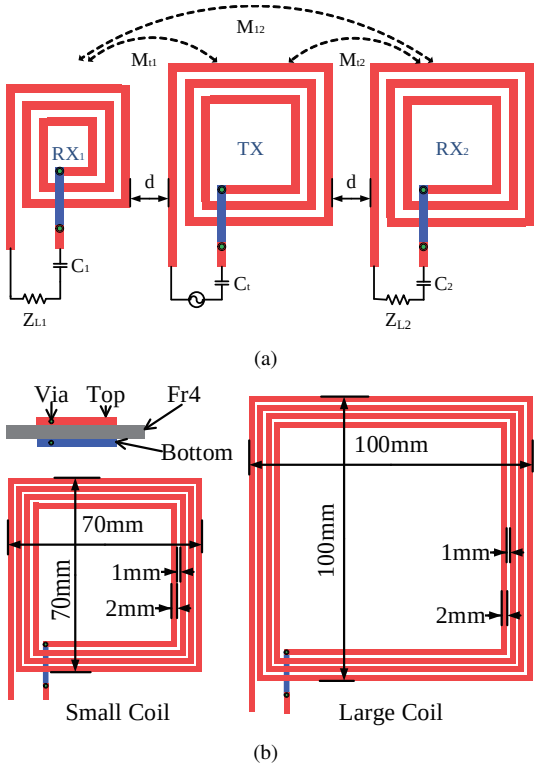

Fig. 4. Coils' layout. (a) Position. (b) Dimension.

TABLE II
MUTUAL INDUCTANCES BETWEEN COILS

d (mm)	M_{t1} (μH)	M_{t2}(μH)	M_{12} (μH)
10	0.130	0.232	0.0071
15	0.113	0.206	0.0066
20	0.094	0.165	0.0063

A. Optimal Loads

Fig. 5 shows the system efficiency when sweeping Z_{L1} and Z_{L2}. The optimal point (triangle in Fig. 5) is $Z_{L1} = 11\ \Omega$, $Z_{L2} = 22\ \Omega$ and $\eta_{OPT} = 0.82$, which lies on the optimal ratio line $Z_{L2} = Z_{L1}R_2/R_1$. If the overall efficiency is the only concern, the maximum power point originally can be found by sweeping each load, which requires strong and intelligent control algorithm. With the conclusion of this paper, the maximum power point tracking for any multiple-receiver system can be easily achieved by sweeping the loads along the optimal ratio line [see Fig. 5] instead of the whole available n-dimensional vector space. However, the designers usually have to consider the available control range for loads. In order to evaluate the influence of loads on efficiency instead of a single optimum point, several constant efficiency contours are plotted in Fig. 5. It shows that there is a range for loads to maintain a significant system efficiency, for example 80%. In order to discuss the influence of the mutual inductances, two different cases are shown in Fig. 6 with different distances. It clearly shows that the optimal point is moving along the optimal ratio line. Besides, larger mutual inductances can provide higher η_{OPT} and allow larger controllable range for Z_{L1} and Z_{L2}.

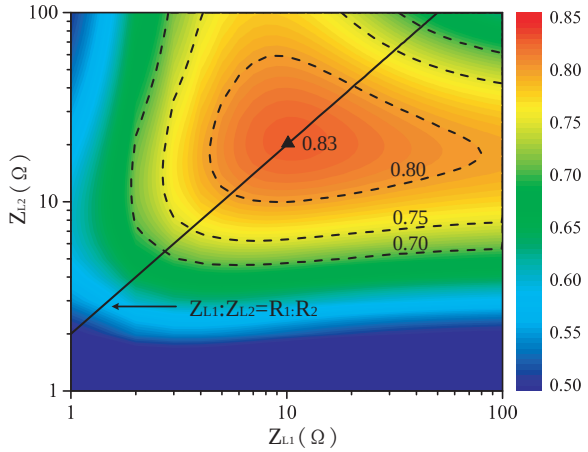

Fig. 5. Efficiency for different loads when d = 15 mm.

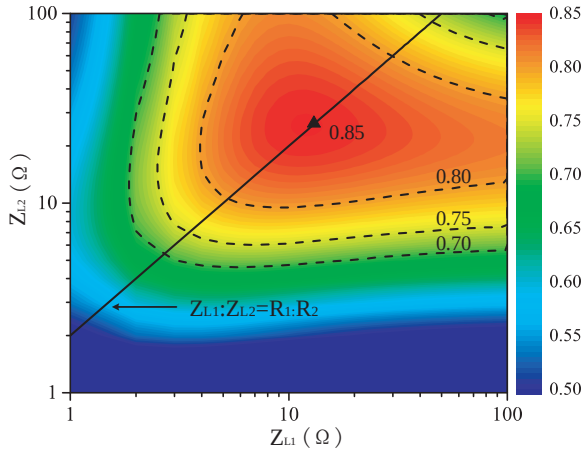

(a)

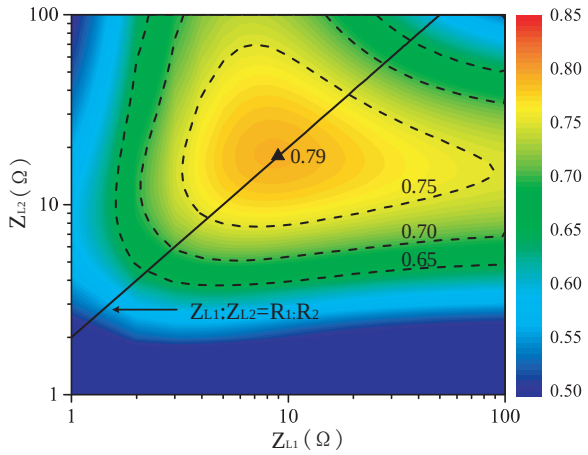

(b)

Fig. 6. The influence of mutual inductances on efficiency. (a) d = 10 mm. (b) d = 20 mm.

B. Input Impedance

It is important to analyze the input impedance of the transmitting coil, because it is the direct load seen by the power source. For a WPT system working at kHz, the inverter usually serves as the power source. According to Z_{IN}, the inverter can achieve various proper control methods and techniques, such

as frequency control, current control, voltage control, or soft-switch operation [24], [25]. For a MHz WPT system, a power amplifier should be used, whose performance highly depends on Z_{IN} [8]. The optimal source impedance can be obtained by $Z_S = Z_{IN}^*$. Currently, most power amplifiers use load-pull method to find the acceptable load range and provides impedance requirement for the circuits after PA. In order to design a well-performed PA for WPT, it is significant to obtain the variation of the loads for PA, i.e. Z_{IN}. Based on (36), it reveals that Z_{IN}, like η, depends on the loads (Z_{Li}), the mutual inductances and the number of receivers. Here, the two-receiver system in Fig. 4 is still served as an example. It shows that the $Z_{IN,OPT} = 22\ \Omega$ under optimal loads [refer to (31)]. If Z_{IN} is required to be a constant value or allowed to vary in some range, such as from 20 to 25 Ω, then the controllable range for the Z_{L1} and Z_{L2} will have the constrains as illustrated by the white lines (constant Z_{IN}) in Fig. 7. It means that the loads can be used to adjust the input impedance to satisfy the requirement of the power source, especially the requirement of reducing the power reflection.

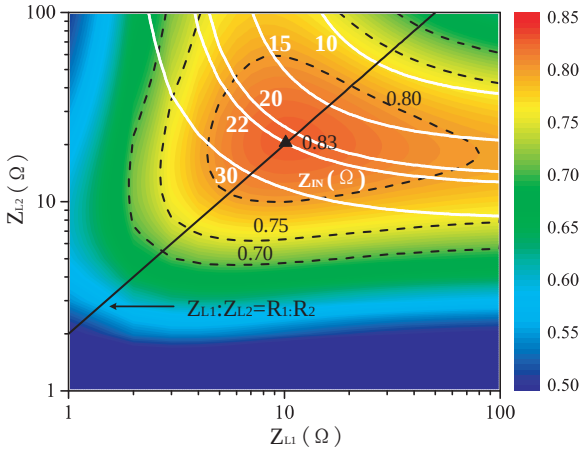

Fig. 7. Constant Z_{IN} curves and efficiency for different loads.

C. Cross Coupling Effects

It is important to consider the influence of cross coupling when the receivers get close to each other. In the original setup [see Table II], the cross coupling M_{12} is negligible compared to M_{t1} and M_{t2}. This simulation evaluates the effects of M_{12} numerically by assigning M_{12} with different value and fixing M_{t1} and M_{t2}. Fig. 5 is again chosen as the reference group. For different M_{12}, the efficiency differences between the original efficiency in Fig. 5 and the efficiencies under cross coupling are given in Fig. 8. The area of negative difference (bounded by the zero-difference curves) means the efficiency decreases under cross coupling. This efficiency drop is small for small M_{12}, even when M_{12} (100 nH) is compatible to M_{t1} (113 nH) and M_{t2} (206 nH). A obvious drop occurs for large M_{12} (400 nH). The same effects have also been observed and evaluated in [28], [32].

In Fig. 8, efficiency improvement can also be observed in narrow regions. These regions correspond to those extreme loading conditions. For example at the point where $Z_{L1} = 50$, and $Z_{L2} = 1$, RX_2 will behave like a repeating coil to enhance the coupling instead of a load extracting power. It means that the cross coupling between RX_1 and RX_2 can actually enhance the equivalent coupling between RX_1 and TX. There are several papers discussing the use of multiple coils to increase system performance [13], [14]. However, in real multiple-receiver systems each receiver is supposed to get power. Therefore, those extreme loading conditions are usually avoided in application.

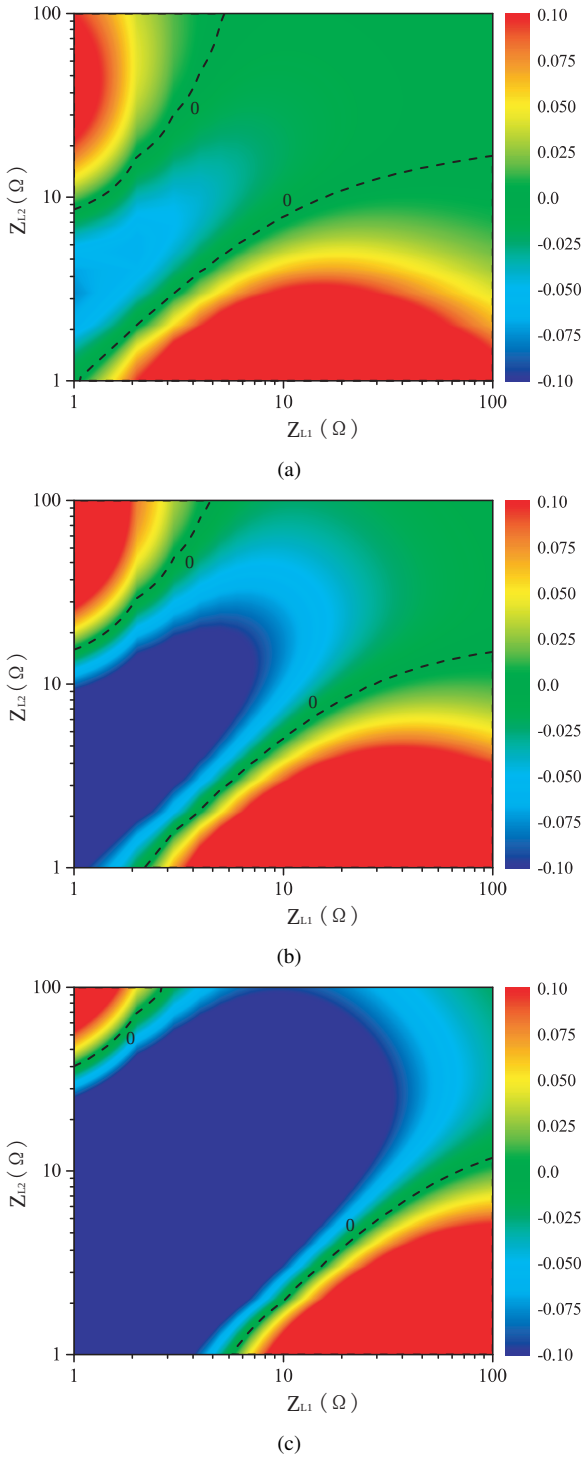

Fig. 8. Efficiency difference under different cross coupling. (a) $M_{12} = 100$ nH. (b) $M_{12} = 200$ nH. (c) $M_{12} = 400$ nH.

IV. Experimental Verification

A. Experiment Setup

The experiments should measure the efficiency for different loads in a multiple-receiver system. A four-port vector network analyzer (VNA), as shown in Fig. 9(a), can be used to measure the system response for at most three receivers. The part number of this VNA is E5071C, Agilent ENA series. With this setup, there are two methods to change the load impedances in the experiment. The first one is to use an internal function of VNA, which is called port-z conversion (PZC). This function can correct the measurement and display the results as if the VNA port impedance had been made into specified values. Actually, this method is a software-based simulator and the physical port impedances are still 50 Ω.

The other method to change load impedance is to use external impedance transformation circuits as shown in Fig. 9(b). An LC circuit is used. In this paper, in order to reduce the parasitic resistance from the LC circuit, the external inductor is avoided. Instead, the inductor for LC circuit (L_{mi}) uses the self inductance of the coil (L_i), and the rest of the self inductance (L_{ri}) is tuned to resonance by C_{ri}. So $L_i = L_{mi} + L_{ri}$. Based on this method, the VNA port impedance 50 Ω can be transformed to the target impedance Z_{target} ($Z_{target} < 50$ Ω) with the following circuit parameters,

$$\begin{cases} C_{mi} = \frac{\sqrt{Z_{target}(50 - Z_{target})}}{50\omega Z_{target}} \\ L_{mi} = \frac{\sqrt{Z_{target}(50 - Z_{target})}}{\omega} \\ C_{ri} = \frac{1}{\omega^2(L_i - L_{mi})} \end{cases} . \tag{55}$$

The parameters of the two size coils [see Fig. 4] have been given in Table I. A three-receiver system is built with the coils. RX_1 uses the small coil and the others use large coils. The basic coils' positions are illustrated in Fig. 9 (c). The transmitter (TX) is placed in the middle, and three receivers (RX_1, RX_2 and RX_3) are localized right around the transmitter with a horizontal distance w. Through different experiments, the measurement rule for the VNA is, Port One for TX, Port Two for RX_1, Port Three for RX_2, and Port Four for RX_3. With the setup in Fig. 9 (a) and (c), the one- or two-receiver systems can be easily defined by removing two or one receiver from the three-receiver system as below.

- One-receiver system: Only TX and RX_1 are used; RX_2 and RX_3 are removed. $\eta = |S_{21}|^2/(1-|S_{11}|^2)$ [see Fig.9 (e)].
- Two-receiver system: TX, RX_1 and RX_2 are used; RX_3 is removed. $\eta = (|S_{21}|^2+|S_{31}|^2)/(1-|S_{11}|^2)$ [see Fig.9 (d)].
- Three-receiver system: All the coils are used. $\eta = (|S_{21}|^2 + |S_{31}|^2 + |S_{41}|^2)/(1 - |S_{11}|^2)$ [see Fig.9 (c)].

For systems with different number of receivers, w is always used to denote the distance between the transmitter and each receiver. By changing w, it can vary the mutual inductances. This planar configuration is sufficient to evaluate the influence of the mutual inductances for a general system with measurement conveniences. In the final experiment, different positions are used and their corresponding mutual inductances are given in Table. III. Three different cases are defined, case A for large mutual inductances, case B for medium mutual inductances and case C for small mutual inductances. This table can give all the mutual inductances for systems with different receivers.

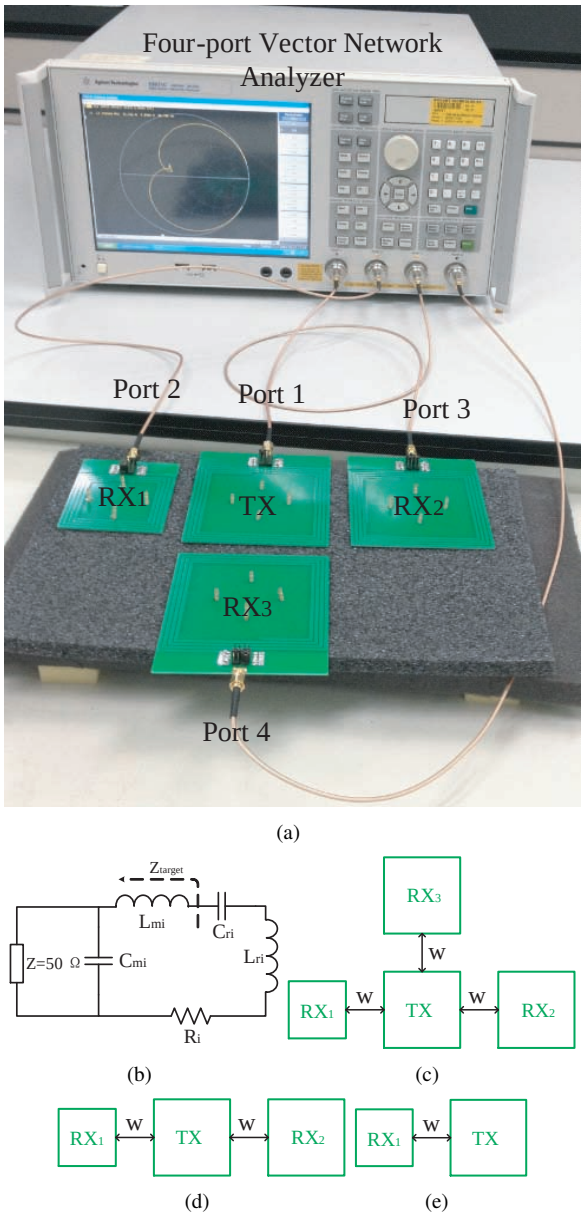

Fig. 9. Experiment setup. (a) Measurement platform for three receivers. (b) LC impedance transformation circuit. (c) Three receivers. (d) Two receivers. (e) One receiver.

TABLE III
Mutual Inductances for Different Positions

Label	w (mm)	M_{t1} (μH)	M_{t2} (μH)	M_{t3} (μH)
A	10	0.130	0.232	0.215
B	15	0.113	0.206	0.187
C	20	0.094	0.165	0.158

B. Influence of Loads and Mutual Inductances

Table IV-VI give the results for three different systems with positions defined by Case B [refer to Section IV-A].

For each table, three different results are given and compared. The first one is obtained through numerical calculation (Cal) given in Section II. The with the given circuit's parameters, it can directly calculate the optimal load resistances, efficiency, input impedance and power division ratio. The second one is obtained by using the VNA's function port-z conversion (PZC), which has been described in Section IV-A. And the last one is using LC circuit to transform the standard port impedance (50 Ω) to the required value [refer to Section IV-A]. Thus the system response comparison under different load impedances can be made and used to validate the numerical analysis. By observation, it can be founded that the optimal impedance ratio ($Z_{S,OPT} : Z_{L1,OPT} : ... : Z_{Ln,OPT}$) equals to the parasitic resistance ratio ($R_t : R_1 : ... : R_n$) as the numerical analysis [see (53)]. Also the overall system efficiency can be improved by increasing the number of receivers.

The influence of receivers' positions (mutual inductances) is shown in Table VII. Here a two-receiver system is tested for Case A, B and C as defined in Table III. It shows that the system efficiency increases as the mutual inductances increase. Instead of the single optimal point in the tables, Fig. 10 gives a global view for a two-receiver system for Case B. It shows the results for Cal, PZC and LC are well matched to each other. The frequency response is given for Case B in Fig. 11. It also shows that the system efficiency is improved by using optimal loads ($Z_{L1} = 11\ \Omega$ and $Z_{L2} = 22\ \Omega$).

TABLE IV
ONE-RECEIVER SYSTEM (CAL: CALCULATION)

	Cal	PZC	LC
$Z_{L1,OPT}$	6.93	6.86	7
$Z_{S,OPT}$	13.67	12.35+3j	12.2+3j
Optimal impedance ratio	1:0.5	1:0.56	1:0.57
η	0.7391	0.7203	0.7201

TABLE V
TWO-RECEIVER SYSTEM

	Cal	PZC	LC
$Z_{L1,OPT}$	10.85	10.9	11
$Z_{L2,OPT}$	22.24	23.3	22
$Z_{S,OPT}$	22.24	21.8+0.8j	22.5+0.8j
Optimal impedance ratio	1:0.5:1	1:0.5:1.07	1:0.5:0.98
η	0.8312	0.8271	0.8268

TABLE VI
THREE-RECEIVER SYSTEM

	Cal	PZC	LC
$Z_{L1,OPT}$	13.58	13.4	13
$Z_{L2,OPT}$	27.84	28.4	28
$Z_{L2,OPT}$	25.13	24.8	25
$Z_{S,OPT}$	27.84	26.4-3.5j	26.6-2j
Optimal impedance ratio	1:0.5:1:0.9	1:0.51:1.08:0.94	1:0.49:1.05:0.94
η	0.8629	0.8537	0.8534

C. Input Impedance and Power Distribution

In order to achieve a target Z_{IN} when Z_{L1} is given, Z_{L2} can be calculated by solving (23). In the experiment, 22 Ω is set to be the target impedance for Z_{IN}. For each Z_{L1}, the required Z_{L2} is shown by the blue line in Fig. 12. Both PZC and LC are used to change the load impedance, and the corresponding input impedances are recorded and shown in Fig. 12. The consistence between experiment results and calculation validates the proposed method to adjust Z_{IN} by controlling loads.

TABLE VII
EFFICIENCY FOR A TWO-RECEIVER SYSTEM WITH DIFFERENT POSITIONS

	Cal	PZC	LC
Case A	0.8508	0.8464	0.8454
Case B	0.8312	0.8271	0.8268
Case C	0.7981	0.7913	0.7908

Fig. 13 gives the power distribution ratio with different load impedance ratio ($Z_{L1} : Z_{L2}$), for a two-receiver system in Case B [refer to Table III]. In the experiment, Z_{L2} is fixed at 10 Ω, and Z_{L1} is adjusted from 10 to 50 Ω. The power distribution ratio can be obtained by

$$P_1 : P_2 = |S_{21}|^2 : |S_{31}|^2. \tag{56}$$

It finds that curves of two kinds of port impedance transformation methods (PZC and LC) are both well matched to the calculation from (49). It is reasonable to manage the power flow in a multiple-receiver system by load control.

D. Cross Coupling Effects

In order to evaluate the cross coupling effects, the experiment setup for two-receiver system [refer to Fig. 9 (d)] is modified by moving RX_2 up to a different plane z = 30 mm as shown in Fig. 14. O_t, O_1 and O_2 are the centers of TX, RX_1, and RX_2 respectively. θ is the angle between O_tO_2 and x axis. During the experiment, O_t and O_1 are fixed and O_2 rotates along a circle from $\theta = 0^o$ to $\theta = 180^o$. M_{12} varies from nearly 0 to 455 nH during the movement. The system efficiencies under different cross coupling are recorded for $Z_{L1} = 11\ \Omega$ and $Z_{L2} = 22\ \Omega$. An efficiency drop is observed and both PZC and LC give consistent results as calculation predicts.

V. CONCLUSION

In this paper, a detailed numerical analysis is carried out on the efficiency analysis of a multiple-receiver system. A circuit-model-based method is first used to derive the optimal loads and source impedance for one-receiver and two-receiver system, based on which, a general multiple-receiver system is further analyzed. Through numerical method, it gives the expression for overall efficiency, derives the optimal loads and source impedances, discusses the power distribution condition and gives the equivalent one-receiver model for any multiple-receiver system. Some numerical results are further illustrated with a two-receiver system, and proper system design and control method are proposed and discussed. Finally, various experiments are carried out to verify the numerical analysis. Future work is to evaluate how to compensate the cross coupling effects, especially the efficiency drop.

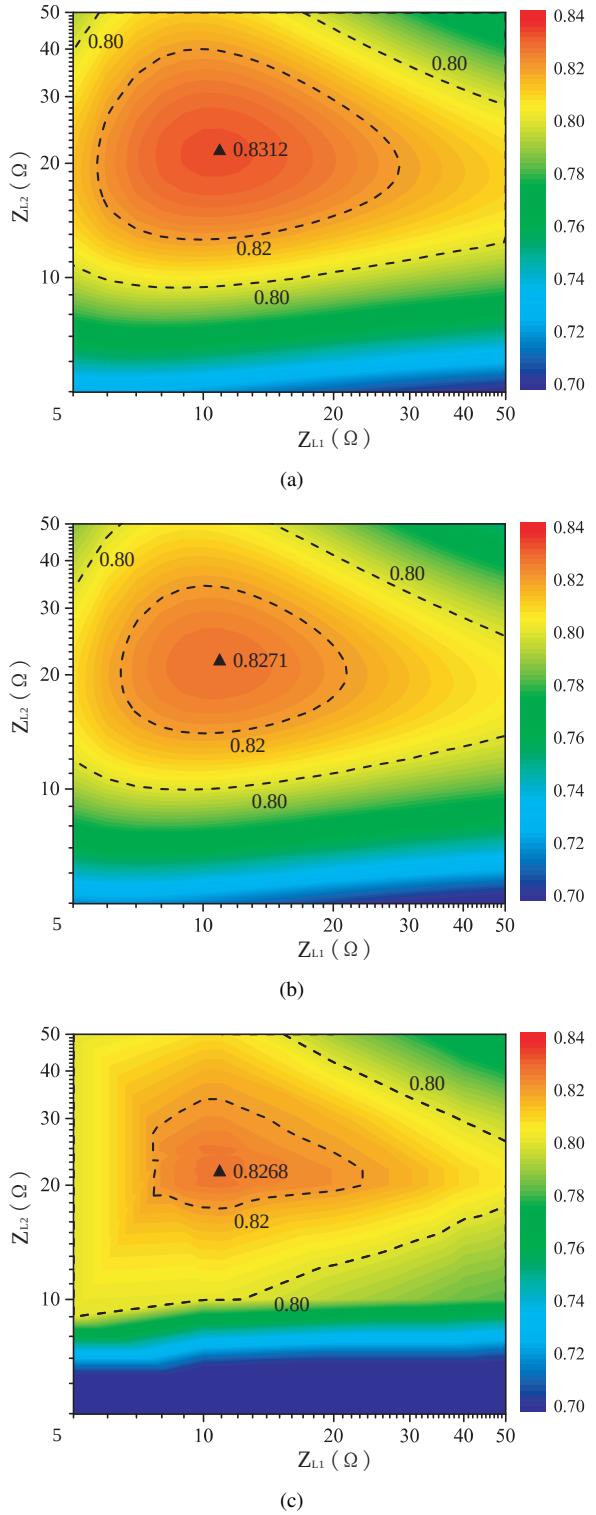

Fig. 10. Efficiency contour comparison with different methods. (a) Cal. (b) PZC. (c) LC.

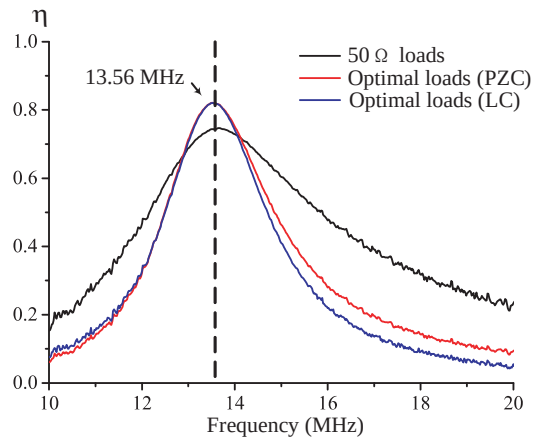

Fig. 11. Efficiency comparison for the two-receiver system in frequency spectrum.

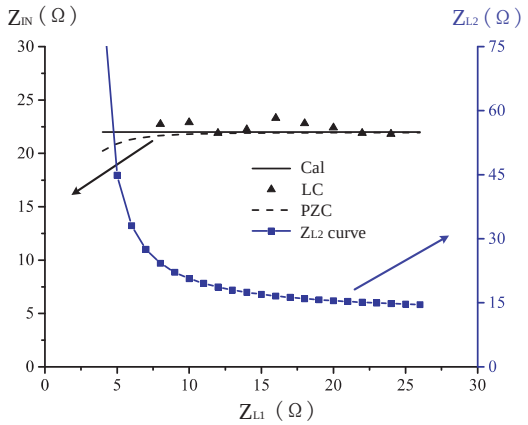

Fig. 12. Constant Z_{IN} curve.

REFERENCES

[1] W. C. Brown, "The history of power transmission by radio waves," *IEEE Trans. Microw. Theory and Techn.*, vol. 32, no. 9, pp. 1230–1242, 1984.

[2] W. C. Brown and E. E. Eves, "Beamed microwave power transmission and its application to space," *IEEE Trans. Microw. Theory Techn.*, vol. 40, no. 6, pp. 1239–1250, 1992.

[3] A. P. Hu, *Wireless/Contactless Power Supply:-Inductively coupled resonant converter solutions*. Saarbrucken, Germany: VDM Publishing, 2009.

[4] A. Kurs, A. Karalis, R. Moffatt, J. D. Joannopoulos, P. Fisher, and M. Soljačić, "Wireless power transfer via strongly coupled magnetic resonances," *Science*, vol. 317, no. 5834, pp. 83–86, 2007.

[5] S. Hui, W. Zhong, and C. Lee, "A critical review of recent progress in mid-range wireless power transfer," *IEEE Trans. Power Electron.*, vol. 29, no. 9, pp. 4500–4511, 2014.

[6] N. Shinohara, "Power without wires," *IEEE Microw. Mag.*, vol. 12, no. 7, pp. S64–S73, 2011.

[7] J. J. Casanova, Z. N. Low, and J. Lin, "Design and optimization of a class-e amplifier for a loosely coupled planar wireless power system," *IEEE Trans. Circuits Syst. II, Exp. Briefs*, vol. 56, no. 11, pp. 830–834, 2009.

[8] S. Aldhaher, P. Luk, and J. Whidborne, "Tuning class e inverters applied in inductive links using saturable reactors," *IEEE Trans. Power Electron.*, vol. 29, no. 6, pp. 2969–2978, 2014.

[9] T. Imura and Y. Hori, "Maximizing air gap and efficiency of magnetic resonant coupling for wireless power transfer using equivalent circuit and neumann formula," *IEEE Trans. Ind. Electron.*, vol. 58, no. 10, pp. 4746–4752, 2011.

[10] A. P. Sample, D. A. Meyer, and J. R. Smith, "Analysis, experimental results, and range adaptation of magnetically coupled resonators for wireless power transfer," *IEEE Trans. Ind. Electron.*, vol. 58, no. 2, pp. 544–554, 2011.

[11] S. W. Park, K. Wake, and S. Watanabe, "Incident electric field effect and numerical dosimetry for a wireless power transfer system using magnetically coupled resonances," *IEEE Trans. Microw. Theory Techn.*, vol. 61, no. 9, pp. 3461–3469, 2013.

[12] M. Q. Nguyen, Z. Hughes, P. Woods, Y.-S. Seo, S. Rao, and J. Chiao, "Field distribution models of spiral coil for misalignment analysis in

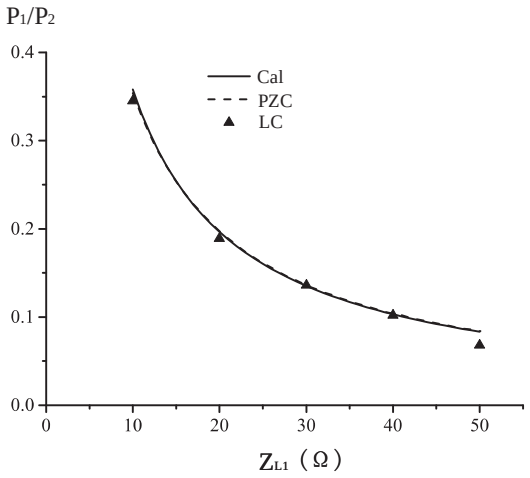

Fig. 13. Power Distribution Ratio for $Z_{L2} = 10\ \Omega$.

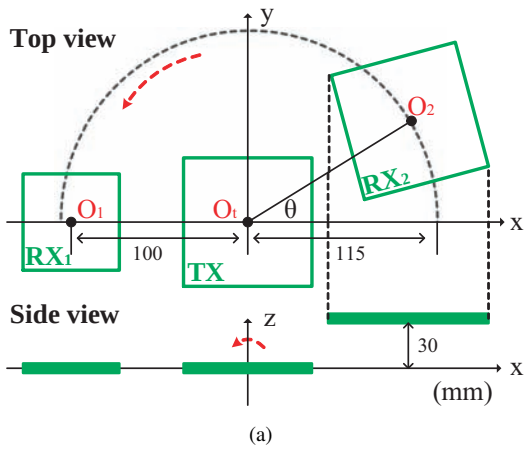

(a)

Fig. 14. Experiment setup for evaluating the cross coupling effects.

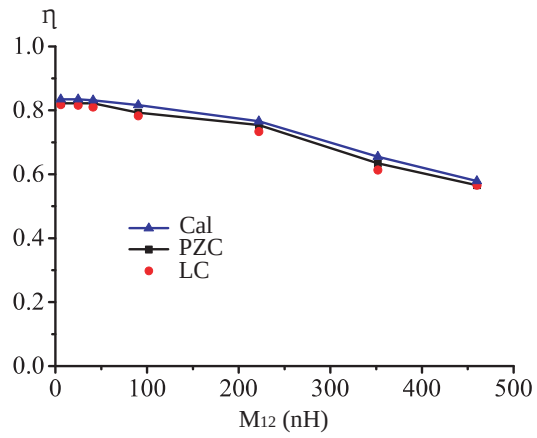

Fig. 15. System efficiency under different cross coupling ($Z_{L1} = 11\ \Omega$ and $Z_{L2} = 22\ \Omega$).

wireless power transfer systems," *IEEE Trans. Microw. Theory Techn.*, vol. 62, no. 4, pp. 920–930, 2014.

[13] M. Kiani, U.-M. Jow, and M. Ghovanloo, "Design and optimization of a 3-coil inductive link for efficient wireless power transmission," *IEEE Trans. Biomed. Circ. Syst.*, vol. 5, no. 6, pp. 579–591, 2011.

[14] F. Zhang, S. A. Hackworth, W. Fu, C. Li, Z. Mao, and M. Sun, "Relay effect of wireless power transfer using strongly coupled magnetic resonances," *IEEE Trans. Magn.*, vol. 47, no. 5, pp. 1478–1481, 2011.

[15] M. Fu, C. Ma, and X. Zhu, "A cascaded boost-buck converter for high efficiency wireless power transfer systems," *IEEE Trans. Ind. Electron.*, vol. 10, no. 3, pp. 1972–1980, 2014.

[16] M. Fu, H. Yin, X. Zhu, and C. Ma, "Analysis and tracking of optimal load in wireless power transfer systems," *IEEE Trans. Power Electron.*, to be pulblished.

[17] Z. N. Low, R. A. Chinga, R. Tseng, and J. Lin, "Design and test of a high-power high-efficiency loosely coupled planar wireless power transfer system," *IEEE Trans. Ind. Electron.*, vol. 56, no. 5, pp. 1801–1812, 2009.

[18] A. Rajagopalan, A. K. RamRakhyani, D. Schurig, and G. Lazzi, "Improving power transfer efficiency of a short-range telemetry system using compact metamaterials," *IEEE Trans. Microw. Theory Techn.*, vol. 62, no. 4, pp. 947–955, 2014.

[19] S. Kim, H.-H. Park, J. Kim, and S. Ahn, "Design and analysis of a resonant reactive shield for a wireless power electric vehicle," *IEEE Trans. Microw. Theory Techn.*, vol. 62, no. 4, pp. 1057–1066, 2014.

[20] D. Krschner and C. Rathge, "Maximizing dc-to-load efficiency for inductive power transfer," *IEEE Trans. Power Electron.*, vol. 28, no. 5, pp. 2437–2447, 2013.

[21] T. P. Duong and J.-W. Lee, "Experimental results of high-efficiency resonant coupling wireless power transfer using a variable coupling method," *IEEE Microw. Compon. Lett.*, vol. 21, no. 8, pp. 442–444, 2011.

[22] J. Park, Y. Tak, Y. Kim, Y. Kim, and S. Nam, "Investigation of adaptive matching methods for near-field wireless power transfer," *IEEE Trans. Antennas Propag.*, vol. 59, no. 5, pp. 1769–1773, 2011.

[23] C. Florian, F. Mastri, R. P. Paganelli, D. Masotti, and A. Costanzo, "Theoretical and numerical design of a wireless power transmission link with gan-based transmitter and adaptive receiver," *IEEE Trans. Microw. Theory Techn.*, vol. 62, pp. 931–946, 2014.

[24] C.-S. Wang, G. A. Covic, and O. H. Stielau, "Investigating an lcl load resonant inverter for inductive power transfer applications," *IEEE Trans. Power Electron.*, vol. 19, no. 4, pp. 995–1002, 2004.

[25] H. H. Wu, G. A. Covic, J. T. Boys, and D. J. Robertson, "A series-tuned inductive-power-transfer pickup with a controllable ac-voltage output," *IEEE Trans. Power Electron.*, vol. 26, no. 1, pp. 98–109, 2011.

[26] A. Kurs, R. Moffatt, and M. Soljačić, "Simultaneous mid-range power transfer to multiple devices," *Applied Physics Letters*, vol. 96, no. 4, p. 044102, 2010.

[27] C.-S. Wang, O. H. Stielau, and G. A. Covic, "Load models and their application in the design of loosely coupled inductive power transfer systems," in *IEEE Int. Conf. Power Syst. Technol.*, vol. 2, Perth, WA, 2000, pp. 1053–1058.

[28] B. L. Cannon, J. F. Hoburg, D. D. Stancil, and S. C. Goldstein, "Magnetic resonant coupling as a potential means for wireless power transfer to multiple small receivers," *IEEE Trans. Power Electron.*, vol. 24, no. 7, pp. 1819–1825, 2009.

[29] K. K. Ean, B. T. Chuan, T. Imura, and Y. Hori, "Impedance matching and power division algorithm considering cross coupling for wireless power transfer via magnetic resonance," in *IEEE 34th Int. Telecom. Energy Conf.*, Scottsdale, AZ, 2012, pp. 1–5.

[30] T. Zhang, M. Fu, C. Ma, and X. Zhu, "Optimal load analysis for a two-receiver wireless power transfer system," in *2014 IEEE Wireless Power Transfer Conf.*, Jeju, 2014, pp. 84–87.

[31] T. C. Beh, M. Kato, T. Imura, S. Oh, and Y. Hori, "Automated impedance matching system for robust wireless power transfer via magnetic resonance coupling," *IEEE Trans. Ind. Electron.*, vol. 60, no. 9, pp. 3689–3698, 2013.

[32] D. Ahn and S. Hong, "Effect of coupling between multiple transmitters or multiple receivers on wireless power transfer," *IEEE Trans. Ind. Electron.*, vol. 60, no. 7, pp. 2602–2613, 2013.

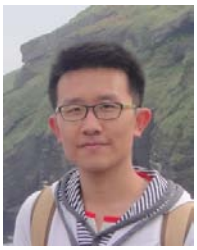

Minfan Fu (S'13) received the B.S. and M.S. degrees both in electrical and computer engineering from University of Michigan-Shanghai Jiao Tong University Joint Institute, Shanghai Jiao Tong University, Shanghai, China in 2010 and 2013, respectively, where he is currently working toward Ph.D. degree.

His research interests include power electronics, control, and their applications in wireless power transfer.

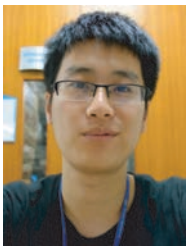

Tong Zhang received the B.S. degree in the electrical and computer engineering from University of Michigan-Shanghai Jiao Tong University Joint Institute, Shanghai, China in 2012. He is currently working toward M.S. degree.

His research interests include the coupling system analysis and the circuit design for wireless power transfer.

Chengbin Ma (M'05) received the B.S.E.E. (Hons.) degree from East China University of Science and Technology, Shanghai, China, in 1997, and the M.S. and Ph.D. degrees both in the electrical engineering from University of Tokyo, Tokyo, Japan, in 2001 and 2004, respectively.

He is currently a tenure-track assistant professor of electrical and computer engineering with the University of Michigan-Shanghai Jiao Tong University Joint Institute, Shanghai Jiao Tong University, Shanghai, China. He is also with a joint faculty appointment in School of Mechanical Engineering, Shanghai Jiao Tong University. Between 2006 and 2008, he held a post-doctoral position with the Department of Mechanical and Aeronautical Engineering, University of California Davis, California, USA. From 2004 to 2006, he was a R&D researcher with Servo Laboratory, Fanuc Limited, Yamanashi, Japan. His research interests include wireless power transfer, networked hybrid energy systems, and mechatronic control.

Xinen Zhu (S'04-M'09) received the B.Eng. (Hons.) degree in electronic and communication engineering from City University of Hong Kong, Hong Kong, in 2003, and the M.S. degree and the Ph.D. degree in electrical engineering from The University of Michigan at Ann Arbor, in 2005 and 2009 respectively.

He is currently a tenure-track assistant professor of electrical and computer engineering with the University of Michigan-Shanghai Jiao Tong University Joint Institute, Shanghai Jiao Tong University, Shanghai, China. His research interests include wireless power transfer, tunable RF/microwave circuits, and ferroelectric thin films.